PIBB 生物化学与生物物理进展
Progress in Biochemistry and Biophysics
2013, 40(4): 333~344
www.pibb.ac.cn

Sll1466, a Glycosyl Transferase Homolog Involved in Stress Response and Regulation of Phosphorylation and Glycosylation Reactions in *Synechocystis* PCC 6803*

WANG Xing[1,2], ZHENG Bing-Hui[1,2], LIU Lu-San[1,2)**], DONG Liang-Liang[3)], ZHAO Kai-Hong[3)], ZHOU Ming[3)]

([1)] *State Key Laboratory of Environmental Criteria and Risk Assessment, Chinese Research Academy of Environmental Sciences, Beijing* 100012, China;
[2)] *State Environmental Protection Key Laboratory of Estuarine and Coastal Environment, Chinese Research Academy of Environmental Sciences, Beijing* 100012, China;
[3)] *State Key Laboratory of Agricultural Microbiology, Huazhong Agricultural University, Wuhan* 430070, China)

Abstract Glycosyltransferases are involved in the biosynthesis of oligosaccharides and polysaccharides. They are presented in both prokaryotes and eukaryotes, and play significant roles in biological processes. We deleted the glycosyltransferase homologue gene, *sll1466*, from *Synechocystis* PCC 6803. Thin-section electron micrographs showed that the mutant *Synechocystis* contained more carboxysomes when grown in the absence of CO_3^{2-} and while more glycogen granules when grown in the presence of 0.5 mol/L NaCl than the wild type *Synechocystis*. Absorption spectra of the mutant grown under different light intensities differed significantly from wild type *Synechocystis*. At the molecular level, the mutant differed from the wild type in 3 aspects: (1) glycosylation of two carbohydrate-selective OprB porins in the thylakoid membrane; (2) phosphorylation of the rod-core linker, CpcG1 (Slr2051), in the supernatant of the thylakoid membrane; and (3) transcriptional variations of genes related to the above changes. These results suggested a profound role for Sll1466 in regulating physiology, metabolism, and energy transfer.

Key words cyanobacteria, mutant, glycogen, rod-core linker, glycosyltransferase
DOI: 10.3724/SP.J.1206.2012.00221

Glycosylation of proteins is a widespread post-translational modification. The formation of glycosylated macromolecules has been studied extensively by Roseman[1] who found that glycosylation of molecules was carried out by specific glycosyltransferases(GT) which catalyse the transfer of specific monosaccharides from an activated monosaccharide nucleotide to a specific glycoprotein, glycolipid, or other acceptor macromolecule [2]. The two superfamilies of GT (named GT-A and GT-B respectively) are sub-divided into 65 clades. GTs are also involved in a number of physiological processes, such as the biosyntheses of glycolipids, polysaccharides, and related components of cell walls[3-4].

Glycosyltransferases are involved in the biosynthesis of oligosaccharides and polysaccharides and act through the transfer of sugar moieties from activated donor molecules to specific acceptor molecules, forming glycosidic bonds. They are presented in both prokaryotes and eukaryotes, and utilize an activated nucleotide sugar as a donor

*This work was supported by grants from The National Natural Science Foundation of China (31070743) and The National Major Project of Water Pollution Control and Prevention Technology (2013ZX07502-001) and The Special Scientific Research Project of Environmantal Protection Public Welfare Industry (201309007).

**Corresponding author.
Tel: 86-10-84915316, E-mail: happyhundan@tom.com
Received: May 7, 2012 Accepted: January 9, 2013

and play significant roles in important biological processes[5]. Glycosyltransferases catalyze the synthesis of carbohydrates and glycoconjugates[6] by transferring an activated mono- or oligosaccharide residue to an existing acceptor molecule for initiation or elongation of the carbohydrate chain.

The physiological, genetic and photosynthetic energy transfer importance of glycosyltransferases have been studied *via* deletion genes encoding glycosyltransferases in *Xanthomonas*[7], *Pseudomonas*[8–12] and *Synechocystis* sp. PCC 6803[13–14]. In *Xanthomonas*, there were glycosyltransferase domains at the N and C terminals of RbfCxoo. The deletion of *rbfCxoo* resulted in enhanced virulence and gene expression in mutant Δ*rbfCxoo* compared to the wild type[7]. Other studies indicate that Rbfc plays an important role in flagellin motility, glycosylation, pathogenicity, sensitization and expression of other biological characteristics[8–11]. In *Pseudomonas*, there are three open reading frames in the glycosylation island, designated *orf1*, *orf2* and *orf3*; *orf1* and *orf2* encode putative glycosyltransferases. Mutants with defects in those open reading frames, Δ*orf1* and Δ*orf2*, secreted nonglycosylated and slightly glycosylated flagellins, respectively. Inoculation tests performed with these mutants and original nonhost tobacco leaves revealed that Δ*orf1* and Δ*orf2* could grow on tobacco leaves and caused symptom-like changes[12]. In *Synechocystis* PCC6803, there is a gene (*slr1166*) putatively encoding pteridine glycosyltransferase. The deletion mutant Δ*slr1166* was unable to produce cyanopterin but only 6-hydroxymethylpterin-h-galactoside, verifying that *slr1166* encodes a pteridine glycosyltransferase, which is responsible for transferring the second sugar glucuronic acid in cyanopterin synthesis. The deletion mutant was affected in its intracellular pteridine content and growth rate, which were 74% and 80%, respectively, of wild type, demonstrating that the second sugar residue is still required for quantitative maintenance of cyanopterin[13]. Our previous study reported that a GT homologue (Sll1466) in the cyanobacterium, *Synechocystis* PCC6803, that belongs to clade GT-4 and is highly homologous to GTs in many bacteria[15]. We found that the N-terminal loop domain of ApcE interacted with Sll1466, and constructed a deletion mutant of *Synechocystis*, Δ*sll1466*. The mutant has a smaller size and higher mobility of phycobilisomes on the thylakoid membrane, and a changed lipid composition of the thylakoid membrane, especially decreased amounts of digalactosyl diacylglycerol. These results indicate a profound regulatory role for Sll1466 in regulating photosynthetic energy transfer[14].

In this study, we focus on the physiology, metabolism, and genetics of the deletion mutant, Δ*sll1466*. Our objectives were to assess whether Δ*sll1466*, relative to wild *Synechocystis*, (1) Contained fewer carboxysomes and glycogen granules; (2) Contained less poly-β-hydroxybutyrate; (3) Responded differently to different light intensities or mediums; and (4) Altered transcriptional regulation, phosphorylation of CpcG1(Slr2051), and glycosylation of carbohydrate-selective OprB porins.

1 Materials and methods

1.1 Bacterial strains, media and growth media

Axenic cells of *Synechocystis* sp. strain PCC 6803, a glucose-tolerant strain provided by the Institute of Hydrobiology, Chinese Academy of Sciences, Wuhan, China, were grown in BG11 medium buffered by N-[Tris (hydroxymethyl)methyl]-2- aminoethanesulfonic acid (TES, 20 mmol/L, pH 8) in Erlenmeyer flasks at 30℃ under continuous light of 10 (LL), 50 (ML), or 200 μmol photons·m^{-2}·s^{-1} (HL). The flasks were bubbled with a continuous stream of 0.03% (*v*/*v*) CO_2 in air, and shaken at 150 r/min[16]. Growth was monitored by measuring the absorbance at 730 nm (A_{730}) by a Lambda 25(Perkin-Elmer) spectrophotometer, the relationship between A_{730} and cell numbers is, cell numbers= $6.87124\times10^6 + 9.46733\times10^7 \cdot A_{730}$.

1.2 Preparation of antibody against Sll1466

All genetic manipulations were carried out according to standard protocols[17]. The transformed BL21 cells containing pET30-derived plasmids of *sll1466* were cultured in LB medium at 18℃, supplemented with kanamycin(30 mg/L). After induction with isopropyl β-D-thiogalactoside (1 mmol/L) for 16 h, the cells were centrifuged at 12 000 *g* for 3 min at 4℃, washed twice with water and stored at –20℃ until use.

Cell pellets were resuspended in ice-cold start buffer potassium phosphate buffer (KPB, 20 mmol/L, pH 7.0) containing NaCl (1 mol/L) and disrupted by sonication for 5 min at 50 W (JY92-II, Scientz Biotechnology, Linbo, China). The suspension was centrifuged at 12 000 *g* for 15 min at 4℃. After centrifugation, the supernatant containing Sll1466 was purified *via* Ni^{2+}-affinity chromatography on chelating Sepharose (Amersham-Pharmacia) developed with the

start buffer (pH 7.0). The tagged protein was eluted with the start buffer supplemented with imidazole (0.5 mol/L). For antiserum production, the tagged Sll1466 was purified by SDS-PAGE. The excised bands were mixed with Freund's adjuvant before injecting into the rabbit. Blood was taken 30 days after the inoculation and the antibodies against Sll1466 were purified by fractionation using ammonium sulfate precipitation.

1.3 Generation of mutants

The mutant was constructed according to Wang[14]. The *sll1466* region and neighboring sequences of ~1 kb were PCR amplified with primers P31 and P32, and the amplified ~3.3 kb fragments were cloned into pBluescript(KS+) *via* *Xba* Ⅰ and *Xho* Ⅰ (Table 1) to yield pBlue-neighboring-*sll1466*. By using the mutation kit (Takara) and mutation primers P33 and P34 containing the cutting sites of *Bam*HⅠ, *Bgl*Ⅱ and *Eco*RⅤ (Table 1), *sll1466* was deleted from pBlue-neighboring-*sll1466* to yield pBlue-neighboring. The pBlue-neighboring and pCOLADuet containing the aphⅡ gene (aminoglycoside 3′ phosphotransferase Ⅱ) conferring kanamycin resistance (KmR) were digested with *Eco*RⅤ, and after purification, ligated to yield pBlue-neighboring-Km. The construct of pBlue-neighboring-Km was checked by sequencing and then used to transform *Synechocystis* cells. Transformants were streaked on BG11 plates containing kanamycin (40 mg/L). Segregation of the mutation was achieved by restreaking 2~3 times on these kanamycin plates. Liquid cultures of the mutants were supplemented with kanamycin(40 mg/L). Complete segregation of the mutant was checked by PCR.

Table 1 Primers for (RT-) PCR

Gene	Primer (5′ - 3′)
ssl2823	P_1: CGCCGTGAGTATGATGGGAGGACGTTG
	P_2: GCCGGGCCGCTATTGCTTATTTTTTGC
sll1464	P_3: ATCATTGGCCAGACTCCCTATTCCCGG
	P_4: CAAAGGCGTTCCAAATTCCAGCGACAG
sll1463	P_5: ATGAGGGAATTGAGCGAAGTGGTGGAT
(*ftsH*)	P_6: GCAAATCGGCTTCGGTAACGCTATCTT
sll1462	P_7: ATCCTGCAACAAAGAGATTAGCTGCCA
(*hypE*)	P_8: CGTAATTGCTCCCCACTGATCATGTCT
sll1461	P_9: TAACTTAAGCAAAGCAAATGGTTATCGCCC
	P_{10}: AGGGCCAAGAACTTAAATTTCCTCAGGATC
sll1459	P_{11}: GATCCCCCTGGTATTGAAGCTCTCTATGA
	P_{12}: GCGGAACTTTGCTTATATCTTATCGGCTTA
sll0184	P_{13}: CCCCGGACCTCCATGACTAAACCAA
	P_{14}: TCGGAGCGAATTCAGTGGCCTAACC
slr1194	P_{15}: GCGGGAAAAATCATGGCCAATCGTACC
	P_{16}: AGCGGGGCTCAAATATAGGGCGTGATG
slr0923	P_{17}: AGCCAAGTGACTACAGCCGAAGCAGCA
	P_{18}: CGCCTAGTTACTGCCGCTGAACACCAC
sll1730	P_{19}: GCGTGGAAGAAGCGGATTTTGACAATGAT
	P_{20}: GCCGCCCGACATAAATATCCGAATTACGT
slr1908	P_{21}: GTACCTTCAATGCGGCTACCCCAGATA
(*oprB*)	P_{22}: CCATGGGGAAGCGATAGAACAACTTGT
slr1841	P_{23}: ACCACCAACATTTTCGACCGGGTTAGC
(*oprB*)	P_{24}: TGGTGGTCTGTTCAGGCTTGGAGATCC
Slr2051	P_{25}: GCGGCCTATCGTCAAATCTTTTTCCAT
(*cpcG1*)	P_{26}: CGATGTTGATATTTTGGGCGGAAACCT
Sll1471	P_{27}: TGCCATGGATAATCTGATCGCCGCAGC
(*cpcG2*)	P_{28}: CGGCGGGATAGGGTTGCTTTTGCCATT
sll0247	P_{29}: TCGCTGATCAGTCTGGGCTTTTTATTG
(*isiA*)	P_{30}: CCAGGGTGTTGACTGCACAGAAATAGG
Δ*sll1466* mutant construction	P_{31}: CTTTCTAGAGGGATTTTGCCATGGGGTTTTAAACA
	P_{32}: CCCCTCGAGTTCCTTTGGCTGTTAGTTTTTTAGTG
	P_{33}: CTGAGATCTGATATCCATTAACGAGCGGGGAAATTG
	P_{34}: TGCGGATCCGTTCATTATTGCTTATTTTTTGCC
slr0966	P_{35}: TTGTCGCTTGTTTTAATGCCCTTCGT
trpA(control)	P_{36}: TTATGTGATGGCCGTTTTCAGTTCCC

1.4 Total membrane and thylakoid membrane preparations

The total membrane fraction was obtained by differential centrifugation[18], and thylakoid membranes were prepared similarly by breaking the cells in the MES buffer (50 mmol/L, pH 6.5) containing $MgCl_2$ (10 mmol/L), $CaCl_2$ (10 mmol/L) and glycerol (25% *w*/*v*)[19–20].

1.5 Protein assay

SDS-PAGE was performed with the buffer system of Laemmli (1970) [21] and stained with Coomassie brilliant blue. To detect glycosylation and phosphorylation, gels were stained using the glycoprotein (Gelcode) and Pro-Q ® diamond phosphoprotein staining kits and the bands were visualized by color or fluorescence. The stained proteins were extracted and then identified by MALDI-TOF mass spectroscopy on a Voyager-DE PRO mass spectrometer (Applied Biosystems, Foster City, CA) by the Fit Gene Guangzhou China. Proteins

were identified by searching in the National Center for Biotechnology Information database using Mascot (www.matrixscience.com). For the location of Sll1466, the protein bands were transferred onto nitrocellulose membranes by electroblotting after SDS-PAGE. The membranes were first incubated with the Sll1466 antibody (see above), then with IgG linked with horse radish peroxidase, and then analyzed using the enhanced chemiluminescence (ECM) kit (R&D systems).

1.6 RNA techniques

Total RNA was extracted using the RNA extraction kit (BioFlux). DNA was removed by treatment with RNA-free DNase Ⅰ (Promega). Real time RT-PCR was run on the RT-PCR apparatus (Applied Biosystems, Foster City, CA) by using the SYBR Green Ⅰ kit (Toyobo)[22]. If not stated otherwise, RT-PCR was run three times with isolated RNAs from independent grown cells, using as control *trpA* that is transcribed similarly in wild type and the mutant: average mRNA amounts were reported +/− standard error, and the variations of mRNA of the wild type were divided by the respective ones of Δ*sll1466*. All (RT-) PCR primers are listed in Table 1.

1.7 Physiological and biochemical characterization

Chlorophyll a concentration were determined by absorption spectroscopy [23]. To determine the glycogen content, the reducing sugars resulting from the acidic hydrolysis of glycogen[24] were assayed with 3, 5-dinitrosalicylic acid (DNS), and the amounts were expressed per cell.

1.8 Electron microscopy

Synechocystis cells were fixed in paraformaldehyde (2.5%) and post-fixed with OsO_4 (1%) in phosphate-buffered saline for 2 h, washed again, dehydrated in graded acetone concentrations (30%, 50%, 70%, 80%, 90%) and embedded into Araldite (SPI). Ultrathin sections were prepared by an ultramicrotome (Leica UC 6), placed on copper grids, stained by uranyl acetate and lead citrate, and studied with a transmission electron microscope (Hitachi H-7650). Ultramicrographs were taken with a CCD camera (Gatan 832).

2 Results

2.1 Identification of Sll1466

Sll1466 was unsoluble when it was isolated from overexpressing *E. coli*. *In vivo*, it is associated with plasma membrane components, since it was located in total membrane fractions other than the thylakoid membrane (Figure 1).

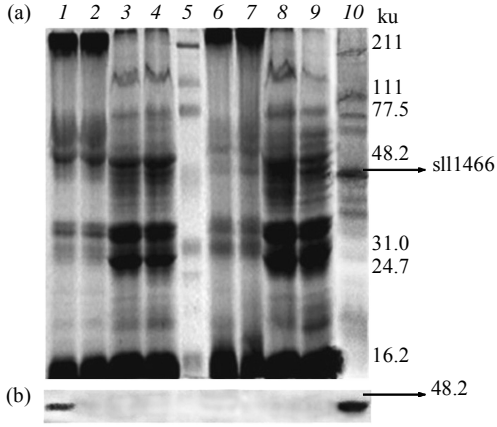

Fig. 1 Localization of Sll1466

(a) SDS-PAGE of total membrane (Tot M) and thylakoid membrane (TM) from *Synechocystis* Δ*sll1466* and wild type. *1*: Tot M from wild type; *2*: Tot M from Δ*sll1466*; *3*: Supernatant of Tot M form wild type; *4*: Supernatant of Tot M from Δ*sll1466*; *5*: Molecular markers; *6*: TM from wild type; *7*: TM from Δ*sll1466*; *8*: Supernatant of TM from wild type; *9*: Supernatant of TM from Δ*sll1466*; *10*: Sll1466 (44 ku) was isolated from overexpressing *E. coli*. (b) Western-blotting of the 44 ku region with the antibody against Sll1466.

2.2 Phenotypic characterization of Δ*sll1466* mutant

To characterize the function of Sll1466, the deletion mutant, Δ*sll1466*, was generated. In standard medium, absorption spectra of Δ*sll1466* differed significantly from wild type under different light conditions (Figure 2), indicating that Δ*sll1466* is involved in light adaptation and, in particular, is more sensitive to HL, which matched the results obtained in our previous study [14]. There was also a qualitative change in absorption: the Chl absorption peak of wild type cells shifted from 683 nm under LL to 680 nm under HL, and that of the phycobiliproteins (mainly phycocyanin, PC) shifted from 630 to 627 nm. In Δ*sl1466*, both blue-shifts were larger: the Chl absorption peak shifted from 683 to 672 nm while that of PC changed from 630 to 622 nm. The blue-shifted Chl absorption under HL has been correlated with the synthesis of IsiA, which is involved in dissipation of excess energy into heat[25]. This is consistent with the result that the transcription of *isiA* is increased by 50% in the mutant during HL growth (Table 2). No such shift has been reported for PC upon induction of

isiA [25]. It is known that the PBS linkers are involved in spectral tuning of the PBS [26], therefore, the blue-shifted PC absorption under HL might relate to the phosphorylation of CpcG1 (Figure 3, Table 3).

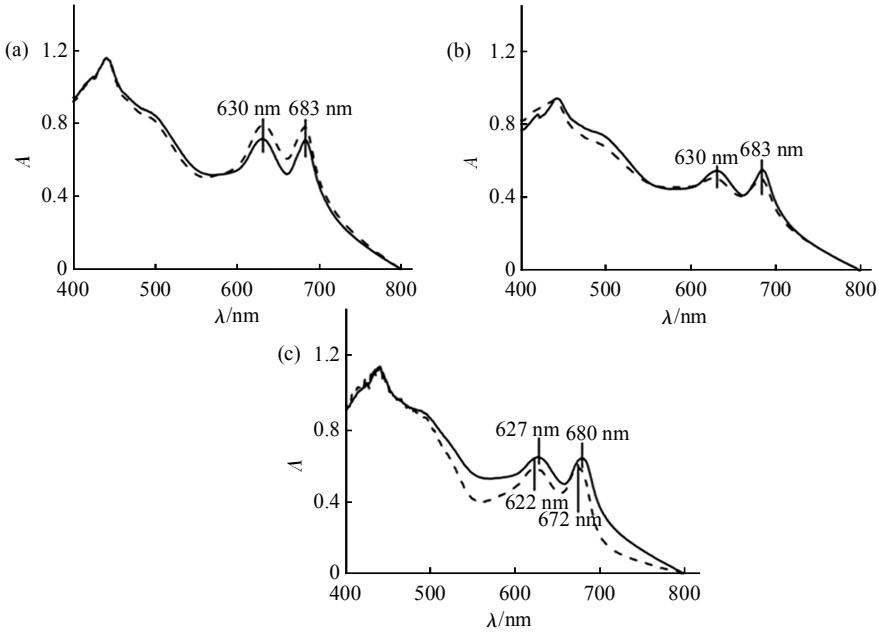

Fig. 2 Absorption spectra of *Synechocystis* grown under different light intensities

The cells of Δ*sll1466* (----) and wild type (——) were grown under LL (a), ML (b), or HL (c) (10, 50 and 200 μmol•m^{-2}•s^{-1}, respectively). Samples were adjusted to Chla 5 mg/L with fresh BG11, and the spectra normalized at 440 nm.

Table 2 Transcriptional effects in Δ*sll1466* mutant: Changes in gene transcripts (wild type/Δ*sll1466*), during phototrophic growth under low (LL), medium (ML) and high light intensities (HL) (see details in Materials and methods)

Gene	Encoded protein	Wild type/Δ*sll1466*		
		LL	ML	HL
ssl2823	Twin-arginine translocation like	0.44 ± 0.02	0.12 ± 0.00	4.0 ± 0.7
sll1464	Hypothetical protein	7.6 ± 0.6	0.03 ± 0.00	0.24 ± 0.07
sll1463 (*ftsH*)	Cell division protein	1.9 ± 0.1	0.02 ± 0.00	0.16 ± 0.04
sll1462 (*hypE*)	Hydrogenase expression/formation	5.4 ± 0.4	0.03 ± 0.00	0.09 ± 0.03
sll1461	Hypothetical protein	1.8 ± 0.1	0.22 ± 0.02	0.54 ± 0.09
sll1459	Stationary phase survival (SurE)	9.9 ± 1.6	0.05 ± 0.00	0.45 ± 0.00
sll0184	RNA polymerase sigma factor (SigC)	0.02 ± 0.00	0.17 ± 0.02	0.08 ± 0.00
slr0923	Similar to a 30S ribosomal protein	0.02 ± 0.00	0.43 ± 0.06	0.21 ± 0.02
sll1730	Hypothetical protein	0.70 ± 0.01	2.2 ± 0.6	0.21 ± 0.07
slr1194	Similar to Mo-dependent Nitrogenase	0.26 ± 0.05	1.3 ± 0.1	0.25 ± 0.03
slr1963	Orange carotenoid protein (OCP)	14 ± 4	17 ± 2	0.25 ± 0.02
slr1908	OprB porin	61 ± 5	0.58 ± 0.03	14 ± 2
slr1841	OprB porin	1.1 ± 0.1	0.17 ± 0.02	1.7 ± 0.2
slr2051 (*cpcG1*)	PBS rod-core linker polypeptide	9.7 ± 0.0	0.14 ± 0.04	3.2 ± 0.4
sll1471 (*cpcG2*)	PBS rod-core linker polypeptide	0.93 ± 0.04	4.2 ± 0.5	0.48 ± 0.04
sll0247	Iron-stress chlorophyll-binding protein	0.20 ± 0.08	220 ± 9	0.66 ± 0.10

Data were generally averaged from three independent experiments.

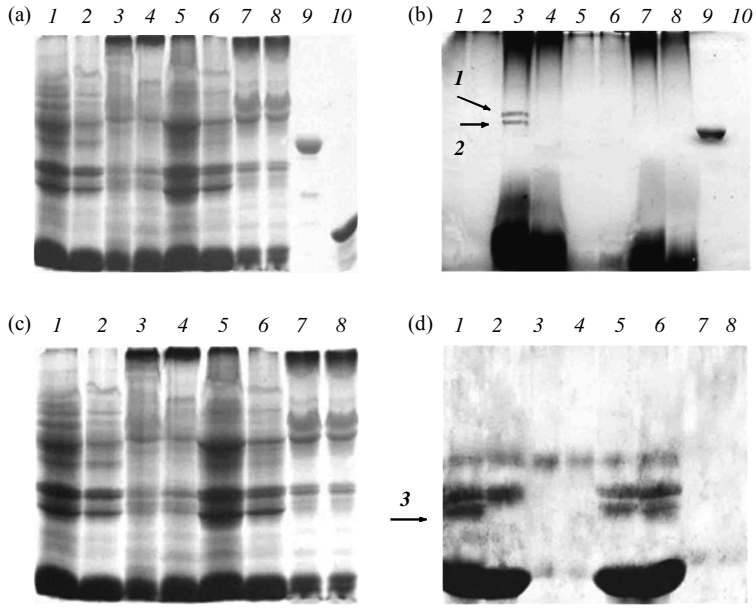

Fig. 3 Differential glycosylation and phosphorylation in Δ*sll1466* and wild type

(a) SDS-PAGE of supernatants of TM from Δ*sll1466* (lane *1*) and wild type (lane *2*), TM from Δ*sll1466* (lane *3*) and wild type (lane *4*), supernatants of Tot M from Δ*sll1466* (lane *5*) and wild type (lane *6*), Tot M from Δ*sll1466* (lane *7*) and wild type (lane *8*), horseradish peroxidase (44 ku, positive control, lane *9*), and soybean insulin (negative control, lane *10*). (b) Same gel as a stained with the glycosylation kit. (c) SDS-PAGE of the same cell fractions as in (a) (lanes *1*～*8*). (d) Same gel as (c) stained for phosphorylation. The arrows indicate the extra bands, which were identified *via* mass spectroscopy as Slr1841 (***1***), Slr1908 (***2***) and Slr2051 (***3***) (see Table 3).

Table 3 Identification and characterization of differentially glycosylated and phosphorylated proteins

Protein (band)	Annotation	MW (*m*/*z*)	P_i	Protein Score / C. I.	Total ion Score / C. I.
Slr1841 (***1***)	OprB protein	67 559.4	4.47	87 / 98.5	56 / 84.8
Slr1908 (***2***)	OprB protein	64 470.9	5.07	357 / 100	256 / 100
Slr2051 (***3***)	LRC CpcG1	27 375.0	9.25	273 / 100	161 / 100

The bands were excised from the gel shown in Figure 3, extracted, and subjected to mass spectroscopy. ***1*** = Upper, ***2*** = Lower marked band in Figure 3b, ***3*** = Marked band in Figure 3d.

The growth of wild type and the mutant were influenced differently by the medium composition: the growth of Δ*sll1466* under ML was slightly faster in the absence of CO_3^{2-} or Cu^{2+}, the difference between wild type and the mutant became negligible in the absence of N or P (Figure 4), and the growth of Δ*sll1466* was inhibited, compared with the wild type, at both high and low pH (Figure 5), as well as in increasing temperature (Figure 6).

The changes in the glycogen concentrations at various light intensities, pH and salt concentrations were similar to the changes in growth rates (Figure 7): adaptation to HL is disturbed in the mutant; the response to high pH in the mutant is opposite to that of the wild type. Glycogen changed only slightly at high NaCl in the wild type, as reported before[27]. Although high salt did not affect growth rates, it resulted in morphological changes that the mutant contained more glycogen granules than the wild type in the presence of 0.5 mol/L NaCl (Figure 8e, f). The number of carboxysomes increased in the mutant, thereby probably compensating for the lack of bicarbonate in

the medium (Figure 8c, d)[28–29]. Conversely, the number of carboxysomes as well as those of glycogen granules and poly-β-hydroxybutyrate in the mutant, relative to wild type, remained similar at low salt (18 mmol/L NaCl) (Figure 8a, b).

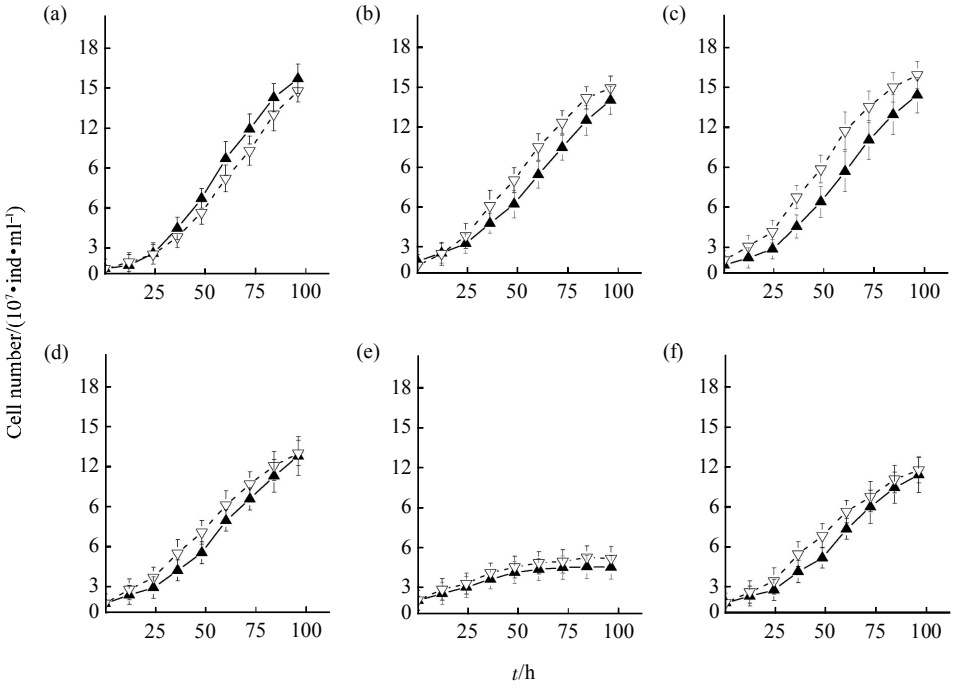

Fig. 4　Growth of *Synechocystis* Δ*sll1466* (▽) and wild type (▲) in limited BG11 media

Cells were grown under 50 μmol photons•m^{-2}•s^{-1} light in BG11 (a), or BG11 with lack of CO_3^{2-} (0.24 *vs*. 0 mmol/L, b), Cu^{2+} (0.002 *vs*. 0 mmol/L, c), Fe^{3+} (0.01 *vs*. 0 mmol/L, d), NO_3^- (17.6 *vs*. 0 mmol/L, e), or HPO_4^{2-} (0.18 *vs*. 0 mmol/L, f). Results are from 3 independent repetitions of the experiments.

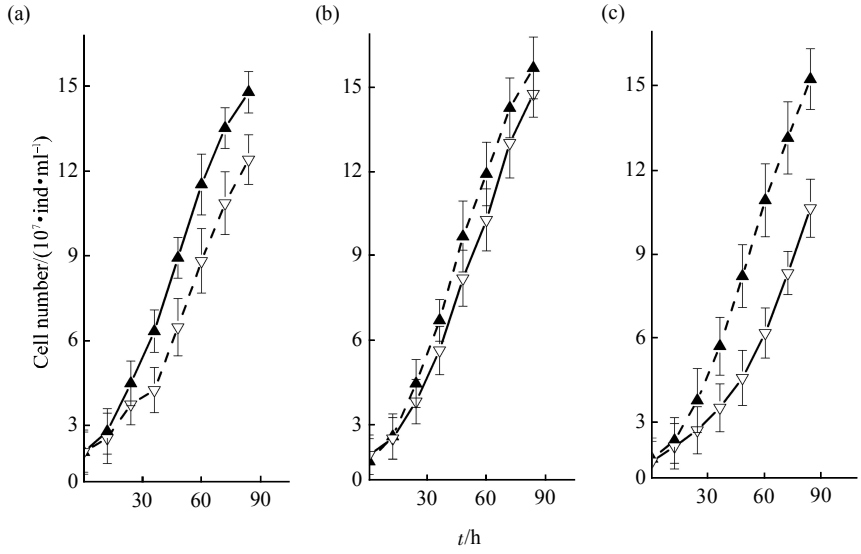

Fig. 5　pH-dependence of growth of *Synechocystis* Δ*sll1466* (▽) and wild type (▲) in BG11 medium under 50 μmol photons•m^{-2}•s^{-1} light

pH = 6.4 (a), 7.5 (b) and 9.0 (c). Results are from 3 independent repetitions of the experiments.

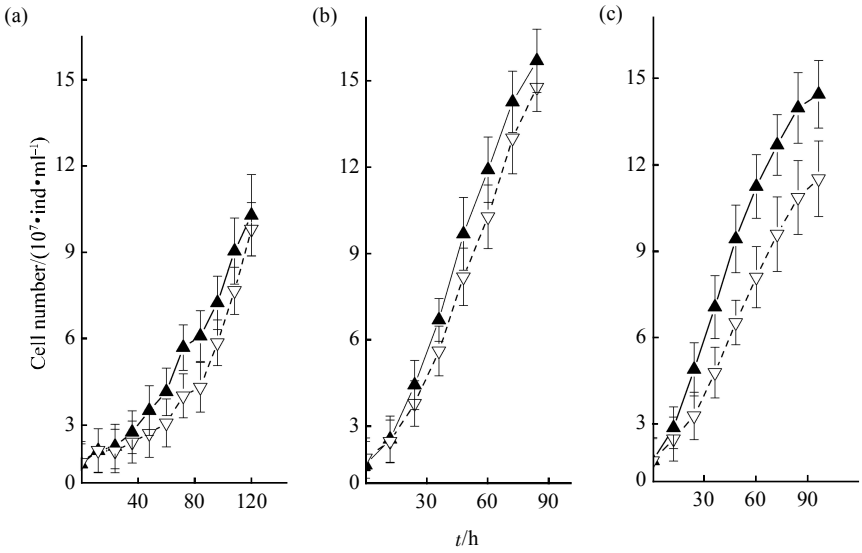

Fig. 6 Temperature dependence of growth of *Synechocystis* Δ*sll1466* (▽) and wild type (▲) in BG11 under 50 μmol photons•m^{-2}•s^{-1} light

T = 20 (a), 30 (b), and 40℃ (c). Results are from 3 independent repetitions of the experiments.

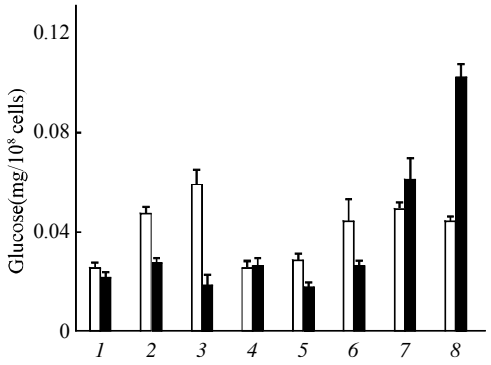

Fig. 7 Glycogen contents in Δ*sll1466* (solid bars) and wild type (open bars)

Cultures were grown in standard BG11 medium (pH 8.0, 18 mmol/L NaCl) under LL (*1*), ML (*2*) and HL (*3*); under ML in BG11 medium at pH 6.4 (*4*) and pH 9.0 (*5*); and under ML in BG11 medium (pH 8.0) containing 0.1 mmol/L NaCl (*6*), 50 mmol/L NaCl (*7*) and 500 mmol/L NaCl (*8*). Results are from 3 independent repetitions of the experiments.

2.3 Altered transcription with the loss of *sll1466*

Transcriptional effects of the deletion of *sll1466* were studied for the contiguous genes, *ssl2823*, *sll1464*, *sll1463*, *sll1462*, *sll1461* and *sll1459*, which are transcribed in the same direction [30] (Table 2). Transcription differences were particularly large for *sll1459*, the transcripts were 19- and 1-fold more abundant, respectively, in the mutant than in wild-type cells during ML and HL growth, but declined by 90% in the mutant during LL growth. The *sll1459* gene encodes stationary phase survival protein, SurE, which improves bacterial viability during stress conditions, and functions as a phosphatase for nucleoside monophosphates [31]. The *ssl2823* transcripts were 1.3- and 7-fold more abundant, respectively, in the mutant than in wild-type cells during LL and ML growth, but declined by 75% in the mutant during HL growth. The *ssl2823* gene encodes a protein similar to twin-arginine translocation protein. Transcript levels of *sll1464* (hypothetical protein), *sll1463* (cell division protein FtsH), *sll1462* (hydrogenase expression/formation protein) and *sll1461* (hypothetical protein) were effected in the opposite way: the *sll1464* transcripts were 32- and 3-fold more abundant, respectively, in the mutant than in wild-type cells during ML and HL growth, but declined by 87% in the mutant during LL growth; the *sll1463* transcrips were 49- and 5-fold more abundant, respectively, in the mutant than in wild-type cells during ML and HL growth, but declined by 47% in the mutant during LL growth; the

sll1462 transcripts were 32- and 10-fold more abundant, respectively, in the mutant than in wild-type cells during ML and HL growth, but declined by 81% in the mutant during LL growth; the *sll1461* transcripts were 4- and 1-fold more abundant, respectively, in the mutant than in wild-type cells during ML and HL growth, but declined by 44% in the mutant during LL growth.

Sll1466 interacts with Sll0184, Slr1194, Slr0923 and Sll1730 [32]. The *sll0184* and *slr0923* transcripts were strongly increased in the mutant; especially during LL growth. The *sll0184* gene encodes the RNA polymerase sigma factor SigC, whereas *slr0923* is similar to a 30 S ribosomal protein. The 50-fold increase of both transcripts during LL growth indicates an involvement of Sll1466 in regulatory networks. Transcripts levels of *sll1730* (encoding a hypothetical protein) and *slr1194* (encoding a protein similar to Mo-dependent nitrogenase family proteins) were comparably less affected in the mutant: the *sll1730* transcripts were 0.5- and 4-fold more abundant, respectively, in the mutant than in wild-type cells during LL and HL growth, but declined by 55% in the mutant during ML growth; the *sll1194* transcripts were 3- and 3-fold more abundant, respectively, in the mutant than in wild-type cells during LL and HL growth, but declined by 23% in the mutant during ML growth (Table 2).

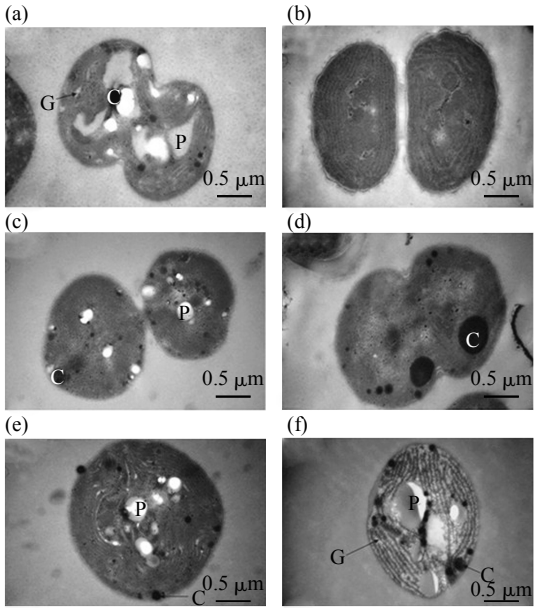

Fig. 8 Thin-section electron micrographs of *Synechocystis* wild type(a,c,e) and Δ*sll1466*(b,d,f) grown phototrophically
Uunder standard conditions of air containing CO_2 (0.03%) (a, b); additionally in the absence of CO_3^{2-} (c, d); and, (e, f) additionally in the presence of 0.5 mol/L NaCl. C, G and P denote carboxysomes, glycogen granules and poly-β-hydroxybutyrate, respectively.

The affected genes, like *slr1908*, coding for membrane components and even more general effects are indicated by the strongly enhanced expression of *sll0184*, *sll1463* and *slr0923* encoding an RNA-polymerase σ-factor (SigC), respectively. SigC is involved, together with SigB and SigD, in the transcriptional regulation of a subset of dark/light-responsive genes in the cyanobacteria[33–36].

2.4 Identification of the regulated components

The dramatic transcriptional changes indicate a strong involvement of Sll1466 in the regulatory cellular network. Therefore, we also studied the glycosylation and phosphorylation of a total membrane fraction and of a thylakoid membrane fraction, and of their respective supernatants. Only a single differential phosphorylation was observed (Figure 3d). The particular protein involved was identified by mass-spectroscopy of the excised band as CpcG1 (Slr2051) (Table 3); the phosphorylated protein appeared only in the supernatant of the thylakoid membrane from the mutant Δ*sll1466*. CpcG1 is one of the rod-core linkers that attach the PBS rods to the core [27, 37–38]. Disassembly of PBS has been associated with the phosphorylation of linkers[39]. A changed PBS structure was also indicated by the reciprocal transcriptional regulation of the two rod-core linker genes, *cpcG1* and *cpcG2* (Table 2).

Two differential glycosylations were detected (Figure 3b), and the respective proteins identified by mass spectroscopy as Slr1908 and Slr1841 (Table 3). Both of them belong to the OprB family and are carbohydrate-selective porins of the outer membrane [40–41]. The two glycosylated OprBs were found, however, in the thylakoid membrane of Δ*sll1466* cells, while OprBs are usually located in the outer membrane and/or plasma membrane [41]. Glycosylation of the two OprBs, induced by the loss of Sll1466, seems to re-directs them to the thylakoid membrane, and thereby could affect carbohydrate transport across the latter. Transcript levels of the two *oprB* genes varied with the light conditions; especially that of *slr1908* decreased by 98% during LL growth in Δ*sll1466* relative to the wild type (Table 2).

3 Discussion

ApcE is one of the two of terminal emitters of the PBS and is critical for ET to PS Ⅱ. As it is also

involved in the organization of the PBS core and in membrane anchoring [19, 42], it is interacting with a considerable number of proteins in the photosynthetic apparatus. In our previous work, Sll1466 was identified as another interaction partner, and the N-terminus of ApcE as the interaction domain. Sll1466 is homologous to glycosyltransferases that are known to affect membrane structure and, indirectly, as well as many other functions[2, 4]. Homologues are presented in other cyanobacteria, indicating similar function in these species. The function of Sll1466, therefore, was studied using a deletion mutant. The deletion is unlikely to cause polar effects at the transcript level because it is the last gene in a cluster, and the direction of transcription changes thereafter[14, 30].

The deletion mutant, Δ*sll1466*, is impaired in acclimatization to HL; the phenotype resembles that of a previously characterized mutant in which the biosynthesis of DGDG is impaired[43]. The reduction of DGDG is less drastic in Δ*sll1466*, but the altered levels of all four major lipids are indicative of a comparable change in membrane structure[14]. This is supported by the increased fluorescence from allophycocyanin(660 nm) and LCM/allophycocyanin-B/CP43(685 nm)[20], which indicate a reduced ET from the PBS to PS Ⅱ. Reduction of Sll0247 (IsiA)[25] also resulted in a similar phenotype (Figure 2, Table 2). Some of the observed changes may, therefore, relate directly to a changed membrane structure just like, the re-localization of carbohydrate-selective porins of the outer membrane to the thylakoid membrane (Figure 3).

Other results, however, indicate that deletion of Sll1466 causes much more profound changes at the transcript levels, protein-protein interaction, and post-translational modification. At the transcript level (Table 2), significant changes are observed in Δ*sll1466* that also depend on the light intensity which the bacteria can grow. Remarkably, there is often no simple correlation with light intensity, but an extreme effect at medium light intensity. It is remarkable that two of the encoded proteins, Sll0184 and Slr0923, are among the interaction partners of Sll1466 [25]. Transcripts levels of *sll0184* and *slr0923* were 50-fold higher during LL growth, so they are two other examples, besides ApcE (reported in our previous study), of transcriptional regulation relating to proteins that interact directly with Sll1466.

Compared with the pleiotropic transcriptional effects, the post-translational effects resulting from deletion of *sll1466* are surprisingly specific, indicating that they may operate early in the interaction network. Glycosylations may relate to the anticipated glycosyl-transferase function of Sll1466. There is, however, also a specific phosphorylation affected, namely, that of CpcG1, which is one of the rod-core linkers that have been related to the size of the PBS and the linkage between the PBSs and the thylakoid membrane [37, 44-46]. Phosphorylation of both rod-core linkers has previously been observed[39, 47], and is related to the disassembly of PBS. Phosphorylation of CpcG1 in Δs*ll1466*, but not in the wild type (Figure 3), may then be directly responsible for the increased mobility and heterogeneity of PBS in the mutant and, thereby, indirectly involved in the changed amplitude and kinetics of state transitions[14].

In summary, two primary actions of Sll1466 can be envisioned from the data obtained in this work. The first is that it is involved in regulatory pathways by specific post-translational phosphorylation and glycosylation reactions. The second relates to its interaction with proteins, including Sll0184 and Slr0923 that are involved in global cellular regulation and stress response.

Acknowledgements We are grateful to R.J. Porra (CSIRO-Plant Industry, Canberra, Australia) and H. Scheer (University Munich, Munich, Germany) for helpful discussions and assistance in preparing the manuscript. We thank GAO Mei, FANG Ping and CHEN Yan for their valuable experimental assistance and R.M. Hughes for English editing.

References

[1] Roseman S. The synthesis of complex carbohydrates by multiglycosyltransferase systems and their potential function in intercellular adhesion. Chem Phys Lipids, 1970, **5**(1): 270-297

[2] Evans I M, Bosmann H B. Glycosyltransferase activity in developing sea-urchin embryos. J Cell Sci, 1977, **25**(1): 355-366

[3] Franco O L, Rigden D J. Fold recognition analysis of glycosyltransferase families: further members of structural superfamilies. Glycobiology, 2003, **13**(10): 707-712

[4] Shao M H, Zheng H Q, Hu Y, *et al*. The GAOLAOZHUANGREN1 gene encodes a putative glycosyltransferase that is critical for normal development and carbohydrate metabolism. Plant Cell Physiol, 2004, **45**(10): 1453-1460

[5] Verbert A, Cacan R. Trafficking of oligomannosides released during N-glycosylation: a clearing mechanism of the rough endoplasmic reticulum. Biochim Biophys Acta, 1999, **1473**(1): 137-146

[6] Laine R A. A calculation of all possible oligosaccharide isomers

both branched and linear yields 1.05×10^{12} structures for a reducing hexasaccharide: the Isomer Barrier to development of single-method saccharide sequencing or synthesis systems. Glycobiology, 1994, **4**(6): 759−767

[7] 孙艳伟, 文景芝, 吴茂森, 等. 糖基转移酶基因 rbfCxoo 缺失突变导致水稻白叶枯病菌毒性表达增强. 微生物学报, 2009, **49**(6): 740−745
Sun Y W, Wen J Z, Wu M S, *et al*. Acta Microbiologica Sinica, 2009, **49**(6): 740−745

[8] Arora S, Bangera M, Lory S, *et al*. A genomic island in *Pseudomonas aeruginosa* carries the determinants of flagellin glycolsylation. Proc Natl Acad Sci USA, 2001, **98**(16): 9342−9347

[9] Taguchi F, Takeuchi K, Katoh E, *et al*. Identification of glycosylation genes and glycosylated amino acids of flagellin in *Pseudomonas syringe* pv. *tabaci*. Cellular Microbiology, 2006, **8**(6): 923−938

[10] Logan S. Flagellar glycolsylation - a new component of the motility repertoire?. Microbiology, 2006, **152**(5): 1249−1262

[11] Verma A, Schirm M, Arora S, *et al*. Glycosylation of b-type flagellin of *Pseudomonas aeruginosa*: structural and genetic basis. J Bacteriology, 2006, **188**(12): 4395−4403

[12] Takeuchi K, Taguchi F, Inagaki Y, *et al*. Flagellin Glycosylation Island in *Pseudomonas syringae* pv. glycinea and its role in host specificity. J Bacteriology, **185**(22): 6658−6665

[13] Hwang Y K, Kang J Y, Woo H J, *et al*. Functional investigation of a gene encoding pteridine glycosyltransferase for cyanopterin synthesis in *Synechocystis* sp. PCC 6803. Biochim Biophys Acta, 2002, **1570**(2): 141−144

[14] Wang X, Dong L L, Zhang C X, *et al*. Sll1466, a glycosyl transferase homolog involved in global cellular regulation and high-light tolerance of *Synechocystis* PCC 6803. Biochem Biophys Res Commun, 2011, **408**(4): 674−679

[15] Altschul S F, Madden T L, Schäffer A A, *et al*. Gapped BLAST and PSI-BLAST: a new generation of protein database search programs. Nucl Acid Res, 1997, **25**(17): 3389−3402

[16] Sokolenko A, Pojidaeva E, Zinchenko V, *et al*. The gene complement for proteolysis in the cyanobacterium *Synechocystis* sp. PCC 6803 and *Arabidopsis thaliana* chloroplasts. Curr Genet, 2002, **41**(5): 291−310

[17] Sambrook J, Fritsch E F, Maniatis T. Molecular Cloning: A Laboratory Manual. Press: New York, Cold Spring Harbour, 1989

[18] Norling B, Zak E, Andersson B, *et al*. 2D-isolation of pure plasma and thylakoid membranes from the cyanobacterium *Synechocystis* sp. PCC 6803. FEBS Lett, 1998, **436**(2): 189−192

[19] Ajlani G, Vernotte C, DiMagno L, *et al*. Phycobilisome core mutants of *Synechocystis* PCC 6803. Biochim Biophys Acta, 1995, **1231**(2): 189−196

[20] Sakurai I, Mizusawa N, Ohashi S, *et al*. Effects of the lack of phosphatidylglycerol on the donor side of photosystem Ⅱ. Plant Physiol, 2007, **144**(3): 1336−1346

[21] Laemmli U K. Cleavage of structural proteins during the assembly of the head of bacteriophage T4. Nature, 1970, **227**(5295): 680−685

[22] Tu C J, Shrager J, Burnap R L, *et al*. Consequences of a deletion in dspA on transcript accumulation in *Synechocystis* sp. Strain PCC 6803. J Bacteriol, 2004, **186**(12): 3889−3902

[23] Laczkó-Dobos H, Ughy B, Tóth S Z, *et al*. Role of phosphatidylglycerol in the function and assembly of Photosystem Ⅱ reaction center, studied in a cdsA-inactivated PAL mutant strain of *Synechocystis* sp. PCC 6803 that lacks phycobilisomes. Biochim Biophys Acta, 2008, **1777**(9): 1184−1194

[24] Valladares A, Maldener I, Muro-Pastor A M, *et al*. Heterocyst development and diazotrophic metabolism in terminal respiratory oxidase mutants of the cyanobacterium *Anabaena* sp. strain PCC 7120. J Bacteriol, 2007, **189**(12): 4425−4430

[25] Wilson A, Boulay C, Kerfeld C A, *et al*. Light-induced energy dissipation in iron starved cyanobacteria roles of OCP and IsiA proteins. Plant Cell, 2007, **19**(2): 656−672

[26] Glazer A N. Adaptive variations in Phycobilisome structure. Adv Mol Cell Biol, 1994, **10**: 119−149

[27] Barker M, Vries R, Nield J, *et al*. The Deg proteases protect *Synechocystis* PCC 6803 during heat and light stresses but are not essential for removal of damaged D1 protein during the photosystem two repair cycle. J Biol Chem, 2006, **281**(41): 30347−30355

[28] Sakuragi Y, Maeda H, DellaPenna D, *et al*. Tocopherol plays a nonantioxidant role in photosynthesis and macronutrient homeostasis of the cyanobacterium *Synechocystis* sp. PCC 6803. That is independent of its antioxidant function. Plant Physiol, 2006, **141**(2): 508−521

[29] Eisenhut M, Wobeser E A V, Jonas L, *et al*. Long-term response toward inorganic carbon limitation in wild type and glycolate turnover mutants of the cyanobacterium *Synechocystis* sp. strain PCC 6803. Plant Physiol, 2007, **144**(4): 1946−1959

[30] Kaneko T, Sato S, Kotani H, *et al*. Sequence analysis of the genome of the unicellular cyanobacterium *Synechocystis* sp. strain PCC 6803. Ⅱ. Sequence determination of the entire genome and assignment of potential protein-coding regions. DNA Res, 1996, **3**(3): 109−136

[31] Pappachan A, Savithri H S, Murthy M R N. Structural and functional studies on a mesophilic stationary phase survival protein (SurE) from *Salmonella typhimurium*. FEBS J, 2008, **275** (23): 5855− 5864

[32] Sato S, Shimoda Y, Muraki A, *et al*. A Large-scale protein − protein interaction analysis in *Synechocystis* sp. PCC 6803. DNA Res, 2007, **14**(5): 207−216

[33] Asayama M, Imamura S, Yoshihara S, *et al*. SigC, the group 2 sigma factor of RNA polymerase, contributes to the late-stage gene expression and nitrogen promoter recognition in the cyanobacterium *Synechocystis* sp. strain PCC 6803. Biosci Biotechnol Biochem, 2004, **68**(3): 477−487

[34] Gunnelius L, Tuominen I, Rantamäki S, *et al*. SigC sigma factor is involved in acclimation to low inorganic carbon at high temperature in *Synechocystis* sp. PCC 6803. Microbiology, 2010, **156**(1): 220−229

[35] Imamura S, Asayama M, Takahashi H, *et al*. Antagonistic dark/light-induced SigB/SigD, group 2 sigma factors, expression through redox potential and their roles in cyanobacteria. FEBS Lett, 2003, **554**(3): 357-362

[36] Tuominen I, Pollari M, Aguirre von Wobeser E, *et al*. Sigma factor SigC is required for heat acclimation of the cyanobacterium *Synechocystis* sp. strain PCC 6803. FEBS Lett, 2008, **582**(2): 346-350

[37] Kondo K, Ochiai Y, Katayama M, *et al*. The Membrane-Associated CpcG2-Phycobilisome in *Synechocystis* A New Photosystem I Antenna. Plant Physiol, 2007, **144**(2): 1200-1210

[38] Sidler W. Phycobilisome and phycobiliprotein structures//Bryant D A. The Molecular Biology of Cyanobacteria. Dordrecht: Kluwer Academic Publishers, 1994, 139-216

[39] Piven I, Ajlani G, Sokolenko A. Phycobilisome linker proteins are phosphorylated in *Synechocystis* sp. PCC 6803. J Biol Chem, 2005, **280**(22): 21667-21672

[40] Wylie J L, Worobec E A. The OprB porin plays a central role in carbohydrate uptake in *Pseudomonas aeruginosa*. J Bacteriol, 1995, **177**(11): 3021-3026

[41] Huang F, Hedman E, Funk C, *et al*. Isolation of outer membrane of *Synechocystis* sp. PCC 6803 and its proteomic characterization. Mol Cell Proteomics, 2004, **3**(6): 586-595

[42] Grossman A R, Schaefer M R, Chiang G G, *et al*. The phycobilisome, a light-harvesting complex responsive to environmental conditions. Microbiol Rev, 1993, **57**(3): 725-749

[43] Mizusawa N, Sakurai I, Sato N, *et al*. Lack of digalactosyldiacylglycerol increases the sensitivity of *Synechocystis* sp. PCC 6803 to high light stress. FEBS Lett, 2009, **583**(4): 718-722

[44] Shen G Z, Boussiba S, Vermaas W F J. *Synechocystis* sp. PCC 6803 strains lacking photosystem I and phycobilisome function. Plant Cell, 1993, **5**(12): 1853-1863

[45] Sarcina M, Tobin M J, Mullineaux C W. Diffusion of phycobilisomes on the thylakoid membranes of the cyanobacterium *Synechococcus* 7942. J Biol Chem, 2001, **276**(50): 46830-46834

[46] Yang S Z, Su Z Q, Li H, *et al*. Demonstration of phycobilisome mobility by the time- and space-correlated fluorescence imaging of a cyanobacterial cell. Biochim Biophys Acta, 2007, **1767**(1): 15-21

[47] Srivastava R, Pisareva T, Norling B. Proteomic studies of the thylakoid membrane of *Synechocystis* sp. PCC 6803. Proteomics, 2005, **5**(18): 4905-4916

蓝细菌 6803 中糖基转移酶 Sll1466 对胁迫响应及其对糖基化、磷酸化反应的调控作用 *

汪 星[1, 2] 郑丙辉[1, 2] 刘录三[1, 2)**] 董亮亮[3] 赵开弘[3] 周 明[3]

([1)] 中国环境科学研究院环境基准与风险评估国家重点实验室，北京 100012；

[2)] 中国环境科学研究院国家环境保护河口与海岸带环境重点实验室，北京 100012；

[3)] 华中农业大学农业微生物国家重点实验室，武汉 430074)

摘要 糖基转移酶存在于原核和真核生物中，参与低聚糖和多糖的生物合成，在生物转化过程中起着重要的作用．本研究中我们去除了 *Synechocystis* PCC 6803 中的糖基转移酶基因 *sll1466*．在不同培养基的光合自养条件下，Sll1466 缺失突变体较野生型的细胞内部结构变化明显(超薄电镜观察)，突变体在缺碳培养基条件下羧酶体含量比野生型高，并且在 0.5 mol/L NaCl 条件下的肝醣含量也明显高于野生型．突变体在不同光密度生长条件下的吸收光谱与野生型差异明显．分子水平上，突变体较野生型显现出如下 3 个方面的差异：a．2 个碳水化合物选择性 OprB 孔蛋白在类囊体膜上发生糖基化；b．核杆连接蛋白 CpcG1(Slr2051)在类囊体膜的上清中发生磷酸化；c．与上述表型差异相关的基因的转录水平亦呈现相同的变化趋势．这些结果预示着 Sll1466 在调控蓝细菌 6803 生理、代谢及能量转化等方面有着重要作用．

关键词 蓝细菌，突变体，糖原，核杆，糖基转移酶

学科分类号 Q2，Q4，Q5 **DOI**: 10.3724/SP.J.1206.2012.00221

* 国家自然科学基金资助项目 (31070743) 和国家水体污染控制与治理科技重大专项 (2013ZX07502-001) 和环保公益性行业科研专项项目 (201309007).

** 通讯联系人.

Tel: 010-84915316, E-mail: happyhundan@tom.com

收稿日期：2012-05-07，接受日期：2013-01-04